Please cite this article as:
Bohdan Mochnacki, Sylwia Lara, Application of generalized finite difference method in numerical modelling of moving boundary problems, Scientific Research of the Institute of Mathematics and Computer Science, 2003, Volume 2, Issue 1, pages 129-143.
The website: http://www.amcm.pcz.pl/

APPLICATION OF GENERALIZED FINITE DIFFERENCE METHOD IN NUMERICAL MODELLING OF MOVING BOUNDARY PROBLEMS

Bohdan Mochnacki, Sylwia Lara

Czestochowa University of Technology, Czestochowa

Abstract. The application of generalized finite difference method for numerical modelling of thermal processes proceeding in the solidifying casting domain is presented. The solidification of pure metals and eutectic alloys is considered. In such case the solidification process takes place at the constant temperature (the Stefan problem). From the numerical point of view the solution of this task is very complex; in particular, in the case of 2D or 3D domains; and in literature one can find the procedures enabling to avoid the difficulties with the direct modelling of the problem discussed. The part of them consist in the substitution of the solidification point T^* by the certain interval $\left[T^* - \Delta T,\ T^* + \Delta T\right]$. In this way the subdomain of artificial mushy zone is introduced and the fixed domain approach [1] can be used. On the stage of numerical algorithm construction and numerical simulation the generalized finite difference method is used. In the final part of the paper the examples of computations are shown.

1. The numerical procedures concerning the Stefan problem (a direct approach)

In the thermal theory of foundry processes two basic macro models of solidification are considered. The first one concern the phase change proceeding at the constant temperature (pure metals and eutectic alloys) while the second one concerns the typical alloys solidifying in the interval of temperature. The sub-domain corresponding to this interval is called the mushy zone sub-domain.

In literature one can find the simple procedures which allow to take into account the solidification process, namely:

- temperature recovery method
- the alternating phase truncation method
- application of the Kirchhoff function
- the certain variation of control volume method.

Here the first of them will be discussed.

1.1. Temperature recovery method

We introduce to the consideration the physical enthalpy of metal defined as follows

$$H(T) = \int_{T_r}^{T} c(\mu)\, d\mu + \eta(T)\, L \tag{1}$$

where for $T > T^*$: $c\,(T) = c_L$ and for $T < T^*$: $c\,(T) = c_S$, while

$$\eta(T) = \begin{cases} 0 & T < T^* \\ 1 & T \geq T^* \end{cases} \tag{2}$$

The course of enthalpy function is shown in Figure 1.

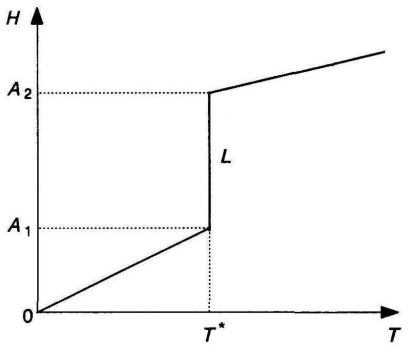

Fig. 1. Enthalpy-temperature function

It should be pointed out that for such mixed enthalpy-temperature convention the formulation of the Stefan condition is needless from the computational view point. If we use the typical numerical algorithm in which the domain is covered by the mesh then if the enthalpy at the node considered x_i i = 1, 2,..., N is from the range [A_1 , A_2] then the temperature T (x_i , t) at this point equals T^*. This value is accepted until $H(x_i, t) < A_1$.

The idea of the temperature recovery method (TRM) is practically the same, but we consider only temperature formulation (it is more convenient on the stage of the numerical algorithm construction). So we introduce the quantity of local temperature reserve z_i defined as follows [1]

$$z_i = \frac{L}{c_L} \tag{3}$$

Using the numerical methods we find the temperatures T_i^f at nodes X_i for successive times t^f, f = 0,1,..., F. If at the moment t^f temperature T_i^f drops below T^* then we accept at this point the temperature T^*, while the temperature reserve is decreased, namely

$$z_i \rightarrow z_i - \left(T^* - T_i^f\right) \tag{4}$$

The same procedure is repeated in successive loops. If for the node x_i $z_i < 0$ we put $z_i = 0$ and next computations are realised without the temperature correction.

The physical interpretation of TRM is the following (see: Fig. 2).

The change of unitary enthalpy corresponding to the change of temperature from T^* to T_i^f found under the assumption that we consider the cooling of molten metal equals

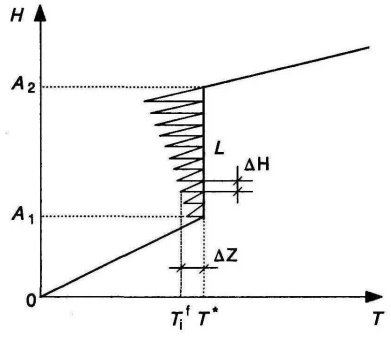

Fig. 2. Interpretation of TRM

$$\Delta H_i = c_L\left(T^* - T_i^f\right) \tag{5}$$

This value we treat as the partial exhaustion' of latent heat L, in particular

$$L \to L - \left(T^* - T_i^f\right) \tag{6}$$

Dividing the last formula by c_L we obtain

$$\frac{L}{c_L} \to \frac{L}{c_L} - \left(T^* - T_i^f\right) \tag{7}$$

The similar approach can be used in the case of solidification in the temperature interval [2].
The remaining procedures mentioned previously are presented, among others, in [3].

2. The numerical procedures concerning the Stefan problem using the artificial mushy-zone

The numerical procedures for which the solidification point is substituted by a certain interval of temperature $\left[T^* - \Delta T,\ T^* + \Delta T\right]$ are the following:

- the Hsiao method
- the modification of the Hsiao method
- application of the Kirchhoff function and enthalpy one
- the artificial heat source method

2.1. The Hsiao method [4]

The Hsiao method bases on the artificial mushy zone (AMZ) introduction. The solidification point is substituted by a temperature interval $\left[T^- = T^* - \Delta T,\ T^+ = T^* + \Delta T\right]$. In this way we can define the substitute thermal capacity of AMZ sub-domain (the slope of the sector between $T^* - \Delta T$ and $T^* + \Delta T$). If we assume the constant values of c_L and c_S then the thermal capacity of the metal is determined by the piecewise function

$$C(T) = \begin{cases} c_L & T > T^* + \Delta T \\ c_P + \dfrac{L}{2\Delta T} & T^* - \Delta T \le T \le T^* + \Delta T \\ c_S & T < T^* - \Delta T \end{cases} \tag{8}$$

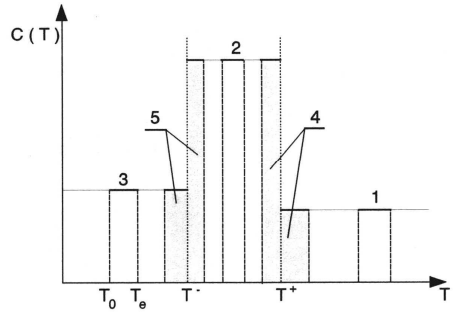

Fig. 3. Thermal capacity of metal

The course of function $C(T)$ is shown in Figure 3.
Let us denote by 0 and e two adjoining points resulting from the domain discretization (node 0 is a central point). We define the thermal capacity c_{0e} in the following way

$$c_{0e} = \frac{1}{T_e - T_0} \int_{T_0}^{T_e} C(T)\,dT \tag{9}$$

and we obtain

$$\begin{aligned}
&T_0,\ T_e > T^+: && c_{0e} = c_L \\
&T_0,\ T_e \in \left[T^-,\ T^+\right]: && c_{0e} = C_P \\
&T_0,\ T_e < T^-: && c_{0e} = c_S \\
&T_0 \in \left[T^-,\ T^+\right],\quad T_e > T^+: && c_{0e} = \frac{c_L\left(T_e - T^+\right) + C_P\left(T^+ - T_0\right)}{T_e - T_0} \\
&T_0 < T^-,\quad T_e \in \left[T^-,\ T^+\right]: && c_{0e} = \frac{C_P\left(T_e - T^-\right) + c_S\left(T^- - T_0\right)}{T_e - T_0} \\
&T_e > T^+,\quad T_0 < T^-: && c_{0e} = \frac{c_L\left(T_e - T^+\right) + C_P\left(T^+ - T^-\right) + c_S\left(T^- - T_0\right)}{T_e - T_0}
\end{aligned} \tag{10}$$

The similar formulas can be found for the case $T_e < T_0$.
Let $e = 1, 2, \ldots, n$ denote indexes of the all adjoining nodes creating the star with the central node 0. Then we define the thermal capacity at the central node as

$$c_0 = \frac{1}{n} \sum_{e=1}^{n} c_{0e} \tag{11}$$

The numerical experiments done by Hsiao and also verified by the authors of above paper show that such approach gives quite good solution of the Stefan problem and the value of interval assumed $[T^-, T^+]$ is not very essential.

2.2. The modification of Hsiao method

In the version presented by Hsiao the numerical algorithm of solidification problem solution is rather complicated. In the paper [5] we present its modification and we show that the definition of c_{0e} results from the following considerations.

One can notice that

$$\int_{T_0}^{T_e} C(T)\,dT = \int_{0}^{T_e} C(T)\,dT - \int_{0}^{T_0} C(T)\,dT = H(T_e) - H(T_0) \tag{12}$$

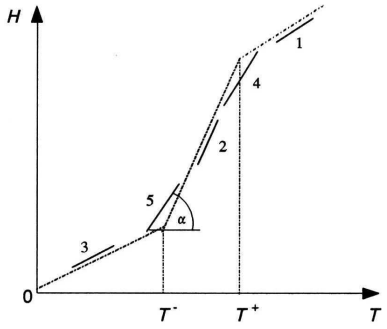

Fig. 4. Thermal capacity c_{0e}

and then

$$c_{0e} = \frac{H(T_e) - H(T_0)}{T_e - T_0} \tag{13}$$

at the same time the relation $T_e > T_0$ or $T_e < T_0$ is here not essential. The interpretation of formula (13) is shown in Figure 4.

2.3. Application of the Kirchhoff function and enthalpy one [6, 7]

We will consider the metal for which the solidification process proceeds partially at the constant temperature and partially in the interval of temperatures. Such situation takes place, among others in the case of cast iron solidification (Fig. 5). The example of the course of enthalpy function for generalized Stefan problem is shown in Figure 6.

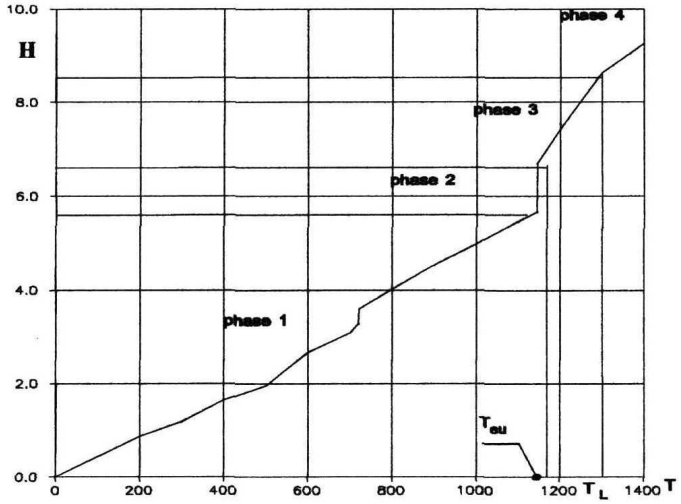

Fig. 5. Enthalpy diagram (cast iron CE = 3.95)

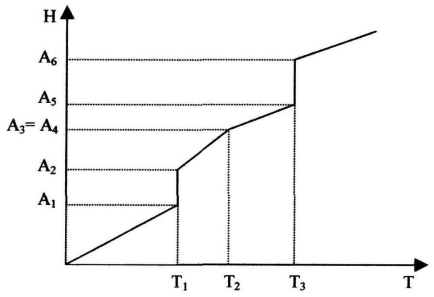

Fig. 6. Generalized course of enthalpy

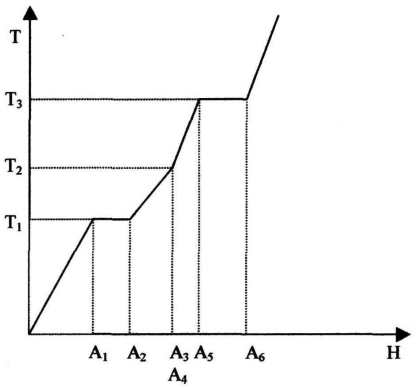

Fig. 7. The inverse function

In such case the function $H(T)$ is determined by the formula

$$H(T)=\begin{cases} A_0 + c_1(T - T_0) & T < T_1 \\ A_2 + c_2(T - T_1) & T_1 \le T < T_2 \\ \vdots & \\ A_{2n-2} + c_n(T - T_{n-1}) & T_{n-1} \le T < T_n \end{cases} \tag{14}$$

We can find the inverse function, namely (see Fig. 7)

$$T(H)=\begin{cases} T_0 + \dfrac{H - A_0}{c_1} & H < A_1 \\ T_1 & A_1 \le H < A_2 \\ T_1 + \dfrac{H - A_2}{c_2} & A_2 \le H < A_3 \\ \vdots & \\ T_{n-1} & A_{2n-3} \le H < A_{2n-2} \\ T_{n-1} + \dfrac{H - A_{2n-2}}{c_n} & A_{2n-2} \le H < A_{2n-1} \end{cases} \tag{15}$$

Now we introduce the Kirchhoff transformation defined as follows (Fig. 8)

$$U(T)=\begin{cases} B_0 + \lambda_1(T - T_0) & T < T_1 \\ B_1 + \lambda_2(T - T_1) & T_1 \le T < T_2 \\ \vdots & \\ B_{n-1} + \lambda_n(T - T_{n-1}) & T_{n-1} \le T < T_n \end{cases} \tag{16}$$

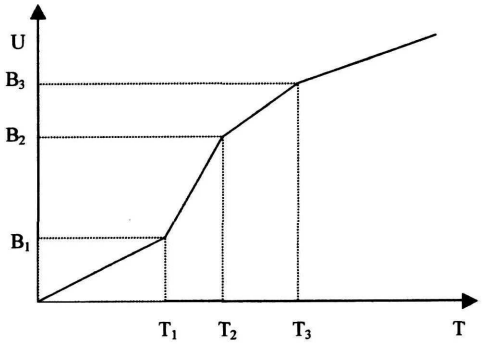

Fig. 8. The Kirchhoff function

where:

$$\begin{aligned} &B_0 = 0, \\ &B_1 = \lambda_1 T_1 = B_0 + \lambda_1 (T_1 - T_0), \\ &B_2 = B_1 + \lambda_2 (T_2 - T_1), \\ &\vdots \\ &B_{n-1} = B_{n-2} + \lambda_{n-1} (T_{n-1} - T_{n-2}) \end{aligned} \tag{17}$$

Finally we can construct the dependence between U and H in the form

$$U(H) = \begin{cases} B_0 + a_1 (H - A_0) & H < A_1 \\ B_1 & A_1 \le H < A_2 \\ B_1 + a_2 (H - A_2) & A_2 \le H < A_3 \\ \vdots & \\ B_{n-1} & A_{2n-3} \le H < A_{2n-2} \\ B_{n-1} + a_n (H - A_{2n-2}) & A_{2n-2} \le H < A_{2n-1} \end{cases} \tag{18}$$

where

$$a_i = \frac{\lambda_i}{c_i} \quad i = 1,2,...,n \tag{19}$$

The course of function $U(H)$ corresponding to the previous figure is shown in Figure 9.
So, the energy equation written in the enthalpy convention is the following

$$\frac{\partial H(x,t)}{\partial t} = \operatorname{div}\{\operatorname{grad}[A(H)H + B(H)]\} \tag{20}$$

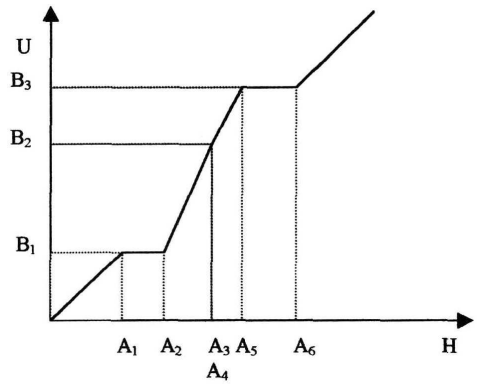

Fig. 9. The dependence between U and H

where

$$A(H)=\begin{cases} a_1 \\ 0 \\ a_2 \\ \vdots \\ 0 \\ a_n \end{cases} \qquad B(H)=\begin{cases} B_0 - a_1 A_0 \\ B_1 \\ B_1 - a_2 A_2 \\ \vdots \\ B_{n-1} \\ B_{n-1} - a_n A_{2n-2} \end{cases} \tag{21}$$

Presented in this paper approach is very convenient for numerical simulation of solidification process both in the case of classical Stefan problem and also for the generalized one.

3. Generalized FDM

On the stage of numerical computations we have used the generalized variant of the FDM. The basic information concerning the way of differential operators approximation and the construction of the numerical algorithm will be presented for the 1D task. So, the following equation

$$c\frac{\partial T(x,t)}{\partial t}=\frac{m\lambda}{x}\frac{\partial T(x,t)}{\partial x}+\lambda\frac{\partial^2 T(x,t)}{\partial x^2}+q_V(x,t) \tag{22}$$

is considered.

The domain is covered by a mesh Δ_h (a set of nodes). Additionally we introduce the time mesh Δ_t defined as follows:

$$0=t^0<t^1<t^2<\ldots<t^{f-1}<t^f<\ldots<t^F<\infty,\ \ \Delta t=t^f-t^{f-1} \tag{23}$$

The cartesian product $\Delta_h \otimes \Delta_t$ creates a spatial-time mesh.

We develop the function $T\left(x, t^{f-1}\right)$ according to the Taylor formula

$$T\left(x,t^{f-1}\right) \cong T\left(x_i,t^{f-1}\right)+\left(\frac{\partial T}{\partial x}\right)_i^{f-1}\left(x-x_i\right)+\left(\frac{\partial^2 T}{\partial x^2}\right)_i^{f-1}\frac{\left(x-x_i\right)^2}{2!} \tag{24}$$

In particular for $x = x_j$ we have

$$T_j^{f-1} = T_i^{f-1} + \left(\partial_x T\right)_i^{f-1}\Delta x_j + \frac{1}{2}\left(\partial_{xx} T\right)_i^{f-1}\Delta x_j^2 \tag{25}$$

where $x_j - x_i = \Delta x_j$. The approximations of the first and second derivatives at the point x_i result from the following quality criterion [4]

$$J = \sum_j \left\{\left[T_i^{f-1} - T_j^{f-1} + \left(\partial_x T\right)_i^{f-1}\Delta x_j + \frac{1}{2}\left(\partial_{xx} T\right)_i^{f-1}\Delta x_j^2\right] w_j\right\}^2 = \min \tag{26}$$

where w_j are the tapering functions. The condition of the minimum functional J is the zeroing of the derivatives $\partial J/\partial (T_x)_i^{f-1}$ and $\partial J/\partial (T_{xx})_i^{f-1}$, and we obtain the system of equations from which the approximation of the first and the second derivatives at point x_i can be found. Using the explicit approach we finally obtain the following equation concerning the internal nodes

$$c\frac{T_i^f - T_i^{f-1}}{\Delta t} = \frac{m\lambda}{x}\Delta_x T_i^{f-1} + \lambda \Delta_{xx} T_i^{f-1} + q_V \tag{27}$$

where Δ_{xx} and Δ_x denote the approximate values of ∂_{xx} and ∂_x. Using this equation one can find the temperature T_i^f. The formulas concerning the numerical form of the boundary conditions and also the stability conditions can be found in [3].

4. Construction of the differential operators [3]

In this part of the paper the examples of the approximations of the first and second derivatives are shown. The 5-points stars (1D task) and the 9-points stars (2D task) have been considered.

In Figure 10 the 5-points stars with different location of the central node is shown.

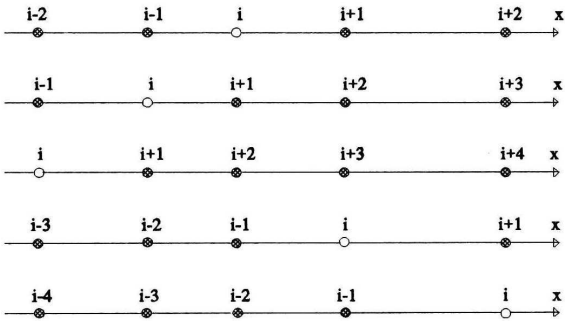

Fig. 10. The 5-points stars

In the case of such stars and different location of the central point we have found the following approximation (the tapering functions w_j are the same):

$$(\partial_x T)_i = \frac{-2T_{i-2} - T_{i-1} + T_{i+1} + 2T_{i+2}}{10\Delta x}, \quad (\partial_{xx} T)_i = \frac{4T_{i-2} + T_{i-1} - 10T_i + T_{i+1} + 4T_{i+2}}{17\Delta x^2}$$

$$(\partial_x T)_i = \frac{-67T_{i-1} + 15T_i + 32T_{i+1} + 29T_{i+2} - 9T_{i+3}}{130\Delta x}, \quad (\partial_{xx} T)_i = \frac{5T_{i-1} - 5T_i - 2T_{i+1} - T_{i+2} + 3T_{i+3}}{13\Delta x^2}$$

$$(\partial_x T)_i = \frac{-270T_i + 127T_{i+1} + 154T_{i+2} + 81T_{i+3} - 92T_{i+4}}{310\Delta x}, \quad (\partial_{xx} T)_i = \frac{10T_i - 7T_{i+1} - 8T_{i+2} - 3T_{i+3} + 8T_{i+4}}{31\Delta x^2}$$

$$(\partial_x T)_i = \frac{9T_{i-3} - 29T_{i-2} - 32T_{i-1} - 15T_i + 67T_{i+1}}{130\Delta x}, \quad (\partial_{xx} T)_i = \frac{3T_{i-3} - T_{i-2} - 2T_{i-1} - 5T_i + 5T_{i+1}}{13\Delta x^2}$$

$$(\partial_x T)_i = \frac{92T_{i-4} - 81T_{i-3} - 154T_{i-2} - 127T_{i-1} + 270T_i}{310\Delta x}, \quad (\partial_{xx} T)_i = \frac{8T_{i-4} - 3T_{i-3} - 8T_{i-2} - 7T_{i-1} + 10T_i}{31\Delta x^2} \tag{28}$$

If we introduce the different values of tapering functions then, for the central position of the central point x_i we have:

- $w_{i-1} = w_{i+1} = 0.3, \; w_{i-2} = w_{i+2} = 0.2$

$$(\partial_x T)_i = \frac{-8T_{i-2} - 9T_{i-1} + 9T_{i+1} + 8T_{i+2}}{50\Delta x}, \quad (\partial_{xx} T)_i = \frac{16T_{i-2} + 9T_{i-1} - 50T_i + 9T_{i+1} + 16T_{i+2}}{73\Delta x^2}$$

- $w_{i-1} = w_{i+1} = 0.4, \; w_{i-2} = w_{i+2} = 0.1$

$$(\partial_x T)_i = \frac{-T_{i-2} - 8T_{i-1} + 8T_{i+1} + T_{i+2}}{20\Delta x}, \quad (\partial_{xx} T)_i = \frac{T_{i-2} + 4T_{i-1} - 10T_i + 4T_{i+1} + T_{i+2}}{8\Delta x^2}$$

- $w_{i-1} = w_{i+1} = 0.35, \; w_{i-2} = w_{i+2} = 0.15$ (29)

$$(\partial_x T)_i = \frac{-18T_{i-2} - 49T_{i-1} + 49T_{i+1} + 18T_{i+2}}{170\Delta x}, \quad (\partial_{xx} T)_i = \frac{36T_{i-2} + 49T_{i-1} - 170T_i + 49T_{i+1} + 36T_{i+2}}{193\Delta x^2}$$

- $w_{i-1} = w_{i+1} = 0.45,\ w_{i-2} = w_{i+2} = 0.05$

$$(\partial_x T)_i = \frac{-2T_{i-2} - 81T_{i-1} + 81T_{i+1} + 2T_{i+2}}{170\Delta x}, \quad (\partial_{xx} T)_i = \frac{4T_{i-2} + 81T_{i-1} - 170T_i + 81T_{i+1} + 4T_{i+2}}{97\Delta x^2}$$

If we consider 2D problem and the star shown in Figure 11 then, for w_j = const:

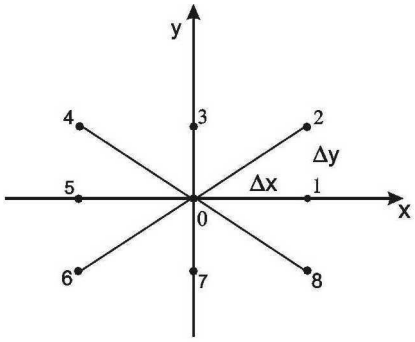

Fig. 11. The 9-points stars

$$\begin{aligned}
(\partial_x T)_0 &= \frac{T_1 + T_2 - T_4 - T_5 - T_6 + T_8}{6\Delta x} \\
(\partial_y T)_0 &= \frac{T_2 + T_3 + T_4 - T_6 - T_7 - T_8}{6\Delta y} \\
(\partial_{xx} T)_0 &= -\frac{6T_0 - 3T_1 - T_2 + 2T_3 - T_4 - 3T_5 - T_6 + 2T_7 - T_8}{5\Delta x^2} \\
(\partial_{yy} T)_0 &= -\frac{6T_0 + 2T_1 - T_2 - 3T_3 - T_4 + 2T_5 - T_6 - 3T_7 - T_8}{5\Delta y^2} \\
(\partial_{xy} T)_0 &= \frac{T_2 - T_4 + T_6 - T_8}{4\Delta x \Delta y}
\end{aligned} \tag{30}$$

The approximation of the Laplace operator we can also find using the control volume method. In particular:

- the equilateral triangle mesh

$$\left(\nabla^2 T\right)_0 = \frac{T_1 + T_2 + T_3 - 3T_0}{0.25h^2} \tag{31}$$

- the hexagon mesh

$$\left(\nabla^2 T\right)_0 = \frac{T_1 + T_2 + T_3 + T_4 + T_5 + T_6 - 6T_0}{4.5h^2} \tag{32}$$

5. Example of computations

We consider the solidification of the rectangular continuous copper casting (1D problem). This problem has been solved using the temperature recovery method (Fig. 12) and the alternating phase truncation method (Fig. 13), using the 5-points stars.

The thermophysical parameters: λ_S = 300 W/mK, λ_L = 300 W/mK, c_S = = 3.746 MJ/m^{3}K, c_L = 4.515 MJ/m^{3}K, L = 1819.68 MJ/m^3, α = 1200 W/m^{2}K (crystallizer of length 0.5 m), α = 800 W/m^{2}K (secondary cooling zone), T_w = = 40°C, T_0 = 1120°C, w = 0.01 m/s.

The comparison of the obtained solutions is shown in Figure 14.

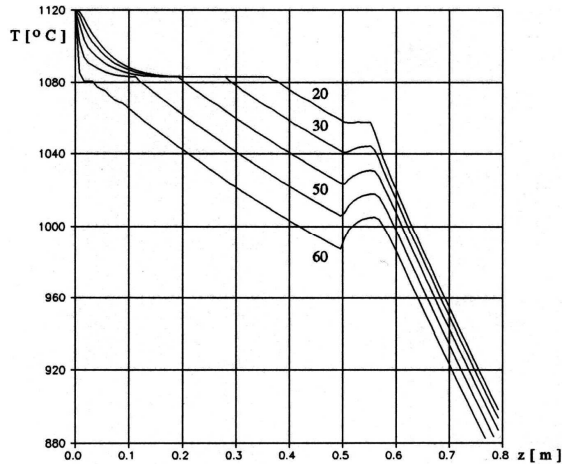

Fig. 12. The solutions on the basis of the TRM

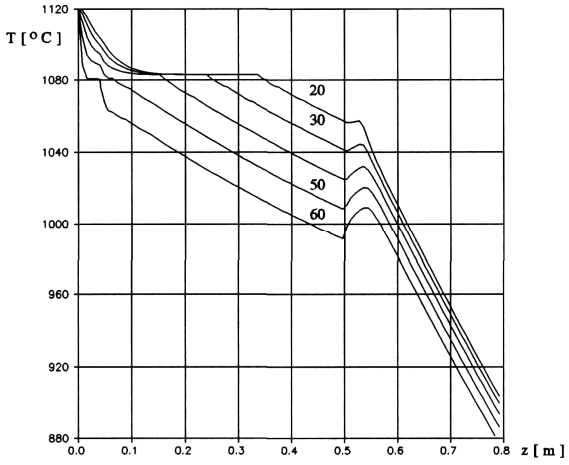

Fig. 13. The solutions on the basis of the APTM

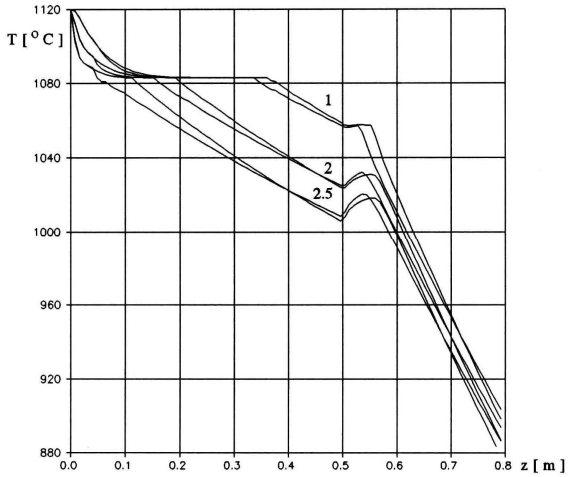

Fig. 14. The comparison of the TRM and APTM

Next we consider the continuous aluminium casting of dimensions 10×30 cm (2D problem), using the Hsiao method ($2\Delta T$ = 6, 8 K) and 9-points stars. Thermophysical parameters are the following: λ_S = 261 W/mK, λ_L = 104 W/mK, c_S = = 2.943 MJ/m^{3}K, c_L = 3.070 MJ/m^{3}K, L = 1053 MJ/m^3, α_1 = 1200 W/m^{2}K (heat transfer coefficient in the crystallizer), α_2 = 900 W/m^{2}K (heat transfer coefficient in the secondary cooling zone), T^* = 660°C, T_0 = 700°C, w = 0.02 m/s.

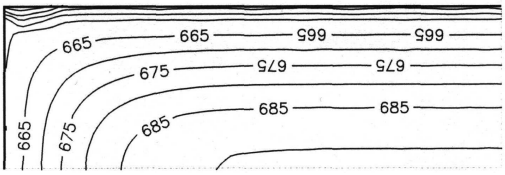

Fig. 15. Temperature field z = 0.2 m, ΔT = 3 K

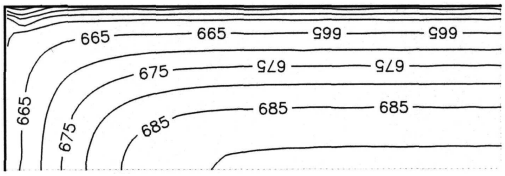

Fig. 16. Temperature field z = 0.2 m, ΔT = 4 K

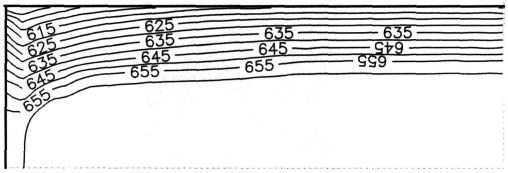

Fig. 17. Temperature field z = 0.8 m, ΔT = 3 K

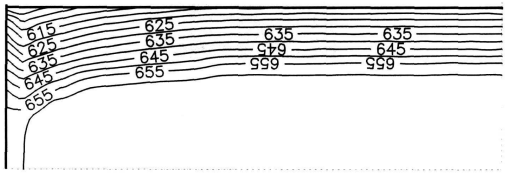

Fig. 18. Temperature field z = 0.8 m, ΔT = 4 K

The non-homogenous domain casting-mould-external chill has been considered. The casting (L-type hot spot) is made from cast iron and produced in the typical sand mould. At the internal corner the square steel chill is located. The dimensions of the system are marked in Figure 19.

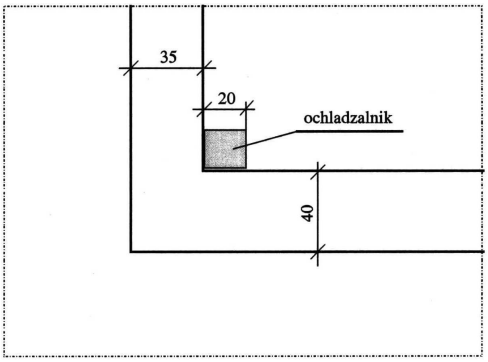

Fig. 19. The non-homogenous domain (casting-mould-external chill)

In Figures 20-23 the obtained temporary positions of isotherms are shown.
The problem has been solved using the application of the Kirchhoff function and enthalpy one.

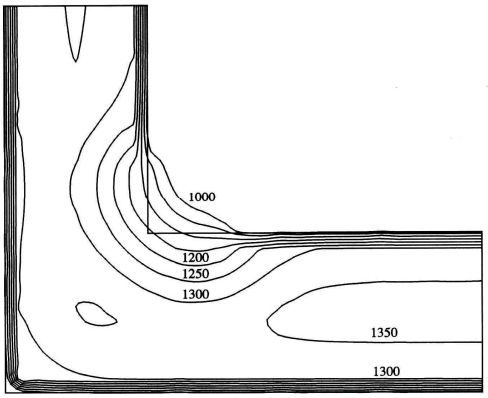

Fig. 20. Temperature field (30 s)

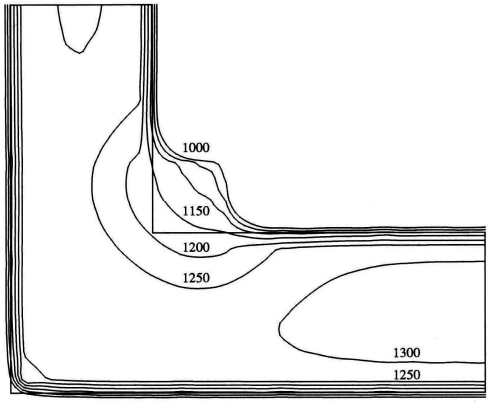

Fig. 21. Temperature field (60 s)

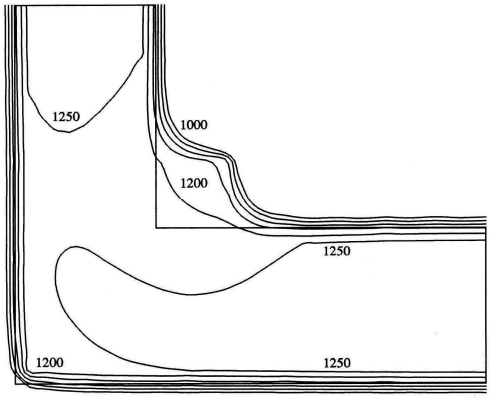

Fig. 22. Temperature field (90 s)

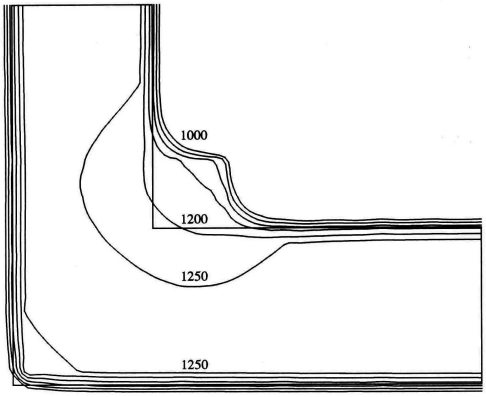

Fig. 23. Temperature field (120 s)

Summing up, the computations done by the authors of the paper show, that the numerical procedures using the AMZ approach are quite effective and exact. The generalized variant of FDM leads to the simple numerical algorithm in particular, if the explicit schemes are taken into account.

References

[1] Mochnacki B., Suchy J.S., Numerical methods in computations of foundry processes, PFTA, Cracow 1995.

[2] Hong C.P., Umeda T., Kimura Y., Numerical models for casting solidification problems, Metal. Trans. 1984, 15B, 101-105.

[3] Lara S., Application of generalized finite difference method in numerical modelling of moving boundary problems, Doctoral thesis, Częstochowa 2003.

[4] Hsiao J.S., An efficient algorithm for finite-difference analyses of heat transfer with melting and solidification, Numerical Heat Transfer 1985, 8, 653-666.

[5] Mochnacki B., Pawlak E., Lara S., Numerical solution of 2D Stefan problem, Solidification of Metals and Alloys 2000, 2, 44, 235-238.

[6] Mochnacki B., Enthalpy approach in numerical modelling of solidification, Part 1, Zeszyty Naukowe Politechniki Opolskiej 2002, Mechanika.

[7] Mochnacki B., Pawlak E., Lara S., Enthalpy approach in numerical modelling of solidification. Part 2, Zeszyty Naukowe Politechniki Opolskiej 2002, 288, Mechanika z. 75, 133-136.

The paper is the part of research BS1-105/301/99/S and BW-05-202/2000/P.